agrochemicals

MDPI

Article

Engineering a Penetratin-Conjugated Soybean Trypsin Inhibitor for Improved Insecticidal Activity Through Oral and Topical Delivery

Sandra San †, Leanie Gracia †, Nikhil Raj Selvaraj, Nandhana Eroth Veedu, Bipin Gopalakrishnan Nair, Jayashree Gopalakrishna Pai, Rajaguru Aradhya and Sudarslal Sadasivan Nair *

Amrita School of Biotechnology, Amrita Vishwa Vidyapeetham, Kollam 690525, Kerala, India
* Correspondence: sudarslal@am.amrita.edu
† These authors contributed equally to this work.

Highlights

- A recombinant soybean trypsin inhibitor-penetratin fusion protein (rSTIP) was developed, expressed in *E. coli*, refolded, purified, and recovered as a functional recombinant protein for insecticidal applications.
- Glutathione-assisted refolding followed by dialysis yielded rSTIP with 65.5% trypsin inhibitory activity relative to the native soybean trypsin inhibitor.
- Oral administration of rSTIP produced stronger developmental inhibition than native soybean trypsin inhibitor in *Drosophila melanogaster*, reducing pupation and adult emergence in a concentration-dependent manner across the tested concentrations in larvae.
- Topical exposure to rSTIP caused complete mortality of *D. melanogaster* larvae within 36 h.

Abstract

Soybean trypsin inhibitor (STI) is a plant defense protein with established activity against insect digestive proteases. In the present study, a recombinant STI-penetratin fusion protein (rSTIP) was developed to evaluate its insecticidal activity following oral and topical exposure. The codon-optimized rSTIP construct was cloned into pET-28a(+) and expressed in *E. coli* BL21(DE3). The recombinant protein was predominantly recovered as inclusion bodies and subsequently solubilized, refolded, and purified using Ni-NTA affinity chromatography. Two refolding strategies were evaluated: on-column refolding and glutathione-assisted dialysis. Glutathione-assisted refolding followed by dialysis resulted in the highest recovery of trypsin inhibitory activity (65.5%). LC-MS/MS analysis provided sequence-level confirmation of the STI component. In *Drosophila melanogaster* larvae, rSTIP exhibited stronger insecticidal activity than the native STI following both oral and topical exposure, with topical application resulting in complete larval mortality within 36 h. Although direct protein penetration or cellular uptake was not evaluated in this investigation, the increased insecticidal activity of STI after conjugation with penetratin suggests improved delivery as a possible mechanism. In the present study, a recombinant STI-penetratin (rSTIP) fusion protein was developed to investigate whether fusion with penetratin could alter the insecticidal activity of STI.

Keywords: soybean trypsin inhibitor; penetratin; cell-penetrating peptide; protein refolding; insecticidal activity

Check for updates

Academic Editor: Guo-Hua Zhong

Received: 15 September 2026
Revised: 19 October 2026
Accepted: 26 October 2026
Published: 30 October 2026

Copyright: © 2026 by the authors. Licensee MDPI, Basel, Switzerland. This article is an open access article distributed under the terms and conditions of the Creative Commons Attribution (CC BY) license.

1. Introduction

Insect pests remain a major constraint to agricultural productivity, causing substantial damage to economically important crops and posing persistent challenges to sustainable crop protection [1]. Although chemical insecticides remain an important component of pest management, their use is associated with environmental concerns and has stimulated the search for safer and more sustainable approaches to insect control [1]. Consequently, increasing attention has been directed toward biopesticides derived from naturally occurring biological molecules, particularly insecticidal proteins, as promising alternatives to conventional insecticides due to their diverse modes of action and potential for selective activity against target pests. The successful application of proteinaceous insecticidal agents, particularly *Bacillus thuringiensis* (Bt) toxins, has demonstrated the feasibility of exploiting biologically derived proteins for crop protection [2]. In addition to microbial toxins, several plant-derived proteins, including lectins, protease inhibitors and amylase inhibitors, have also been investigated for their insecticidal potential, thereby expanding the repertoire of protein-based molecules available for sustainable pest management [3].

Protease inhibitors (PIs) are important plant defense proteins that can interfere with insect digestive physiology by inhibiting proteolytic enzymes required for the digestion and utilization of dietary proteins [4]. Plant protease inhibitors belonging to the family Leguminosae (legumes), Solanaceae (nightshades), and Poaceae (grasses) are among the most studied PIs of the plant kingdom [5]. Among these plant sources, legumes are considered particularly important sources of PIs, owing to the diversity of protease inhibitors accumulated as part of their defense responses against biotic stresses [4]. Depending on the catalytic class of the target proteases and the nature of their active sites, protease inhibitors can be broadly classified into serine, cysteine, aspartic, and metalloprotease inhibitors. Serine protease inhibitors are particularly well studied and are widely distributed in legumes, where Kunitz and Bowman-Birk inhibitors represent two major families [6]. Their ability to inhibit digestive serine proteases makes these inhibitors particularly relevant to plant defense against herbivorous insects. In insects, digestive serine and cysteine proteases represent important targets of plant-derived PIs, and inhibition of these enzymes can impair protein digestion, amino acid availability, growth, and development [7]. The effectiveness of PIs as insecticidal proteins is therefore closely associated with their ability to interfere with the proteolytic machinery of the insect gut [8].

Among legume-derived serine protease inhibitors, soybean trypsin inhibitor (STI), particularly the Kunitz-type inhibitor, has been extensively investigated for its ability to inhibit insect digestive proteases and influence insect development [9]. STI inhibits trypsin and trypsin-like digestive proteases in the insect gut, thereby interfering with proteolytic digestion of dietary proteins [9,10]. STI-mediated inhibition of digestive proteases can impair protein digestion and nutrient utilization, thereby affecting larval growth and development [10]. Consistent with this mechanism, dietary and plant-expressed STI have been reported to reduce larval weight gain, retard larval development, impair pupation, and increase mortality in several lepidopteran pests [10–12]. The insecticidal activity of STI is therefore closely associated with its ability to reach the target site within the insect and effectively interact with its digestive protease targets following ingestion. As a protein-based insecticidal molecule, however, STI may also be subject to limitations associated with its delivery and uptake within the target organism. These considerations highlight the importance of exploring strategies that can improve the delivery and biological availability of protein-based insecticidal molecules.

Although plant protease inhibitors are commonly investigated for their effects on digestive proteases, protease-dependent physiological processes in insects extend beyond the digestive tract. Serine protease cascades in insect hemolymph participate in innate

immune responses, including the activation of prophenoloxidase and pathways involved in antimicrobial peptide production. If a protease inhibitor reaches the hemocoel, it may therefore influence systemic physiological pathways in addition to digestive processes [13,14]. However, whether plant-derived protease inhibitors can exert such effects following topical exposure depends on their ability to cross the insect cuticle and reach internal tissues. This possibility provides an additional rationale for investigating delivery strategies that may alter the biological effects of protein-based insecticidal molecules.

Cell-penetrating peptides (CPPs) are short peptide sequences that facilitate the cellular uptake and intracellular delivery of proteins, peptides, nucleic acids, and other macromolecular cargoes that would otherwise have limited ability to cross biological membranes [15]. The cellular uptake of CPP-cargo complexes is influenced by the physicochemical properties of both the CPP and its cargo, as well as by the characteristics of the target cell [16]. CPP-cargo complexes can enter cells through different uptake pathways, with endocytosis being a major route for the internalization of CPPs conjugated to larger cargoes such as proteins [15,16]. Among the various CPPs identified to date, penetratin is a 16-amino-acid protein-derived CPP originating from the third helix of the Drosophila Antennapedia homeodomain, which was identified as necessary and sufficient for translocation across biological membranes [17,18]. Penetratin has been demonstrated to facilitate the intracellular delivery of hydrophilic molecules, including oligopeptides and oligonucleotides, highlighting its potential as a molecular delivery vector [19]. Penetratin-mediated cellular uptake has been reported to occur through endocytic pathways, including macropinocytosis, supporting its role in the internalization of associated cargoes [20,21]. The incorporation of CPPs into protein-based insecticidal molecules therefore represents a potential strategy to enhance their cellular uptake and improve their delivery to target tissues.

Despite the demonstrated insecticidal potential of protein-based biopesticides, their efficacy can be limited by restricted absorption and cellular uptake within target organisms. Cell-penetrating peptides offer a promising approach to address this delivery limitation by facilitating the transport of protein-based molecules across biological membranes. The study further examined whether CPP incorporation could enhance the biological efficacy of STI following oral and contact-based delivery. Among the available CPPs, penetratin was selected for fusion with STI because of its reported ability to facilitate cellular uptake of associated molecular cargoes. In the present study, STI was fused to penetratin through a flexible peptide linker to investigate whether incorporation of the CPP could alter the biological activity of STI. The fusion architecture was designed to retain the protease-inhibitory function of STI while incorporating penetratin as the CPP moiety within a single recombinant molecule.

The incorporation of a flexible linker between the functional domains of a fusion protein can provide spatial separation and reduce potential interference between the linked domains, thereby supporting their independent folding and biological functions [22,23]. Flexible linkers are particularly useful when two functional domains are required to retain their individual structural and biological properties within a single fusion protein [22,24]. In addition, flexible linkers have been shown to be useful in CPP-protein fusions, where incorporation of a glycine-rich linker improved recombinant expression without compromising cellular translocation of the CPP-cargo fusion [25]. Although CPPs have been extensively investigated as delivery systems for macromolecular cargoes, their application for enhancing the delivery of protein-based insecticidal molecules remains relatively unexplored. To address this, the present study employed penetratin as a CPP to generate a recombinant penetratin-conjugated STI fusion protein and evaluated its insecticidal activity. The study further examined whether CPP incorporation could enhance the biological efficacy of STI following oral and contact-based delivery.

2. Materials and Methods

2.1. Materials

Escherichia coli DH5α and *E. coli* BL21(DE3) strains were obtained from the in-house strain repository. The codon-optimized STI-penetratin gene construct cloned into the pET-28a(+) expression vector was procured from Synbio Technologies (Monmouth Junction, NJ, USA). Ni-NTA resin was purchased from G-Biosciences (St. Louis, MO, USA), while trypsin and Nα-Benzoyl-DL-arginine 4-nitroanilide hydrochloride (BApNA) were procured from Sigma-Aldrich, St. Louis, MO, USA.

2.2. Construction of the STI-Penetratin Fusion Gene

The amino acid sequence of soybean trypsin inhibitor (STI) was obtained from the UniProt database (accession no. P01070). The recombinant construct was designed to contain an N-terminal His_6-tag followed by a TEV protease recognition site, the STI sequence, a flexible G_8 linker, and penetratin at the C-terminus. The corresponding 689 bp gene construct was codon-optimized for expression in *Escherichia coli*, commercially synthesized by Synbio Technologies, and cloned into the pET-28a(+) expression vector using the NcoI and XhoI restriction sites. The recombinant plasmid was supplied as a lyophilized preparation and subsequently used for transformation and heterologous expression in *E. coli*.

2.3. Expression of the Recombinant STI-Penetratin Fusion Protein

The recombinant pET-28a(+) plasmid was transformed into chemically competent *E. coli* DH5α cells by the heat-shock method [26]. Following confirmation of the recombinant plasmid through Sanger sequencing, the construct was transformed into *E. coli* BL21(DE3) cells for protein expression. Transformed cells were cultured in Luria-Bertani (LB) medium supplemented with a final concentration of 50 µg/mL kanamycin at 37 °C. Once the culture reached an OD_{600} of 0.6, protein expression was induced by the addition of 0.5 mM IPTG, followed by incubation at 16 °C for 8 h. Cells were harvested by centrifugation at 6000 rpm for 15 min at 4 °C. The cell pellet was resuspended in 20 mM Tris-HCl buffer (pH 8.0) containing 500 mM NaCl, 2 M urea, and 2% (*v*/*v*) Triton X-100, followed by sonication on ice for cell lysis. The lysate was centrifuged at 6000 rpm for 10 min at 4 °C to separate the soluble and insoluble fractions. The insoluble fraction containing the recombinant STI-penetratin (rSTIP) fusion protein was subsequently washed with the same buffer without urea, followed by washing with 20 mM Tris-HCl (pH 8.0) containing 500 mM NaCl. After each washing step, the sample was centrifuged, and the supernatant was discarded. The resulting pellet, enriched in the rSTIP in the form of inclusion bodies, was retained for subsequent solubilization.

2.4. Solubilization and Refolding of rSTIP Fusion Protein

2.4.1. Solubilization of Inclusion Bodies

The isolated inclusion bodies were dissolved in a solubilization buffer containing 20 mM Tris-HCl (pH 8.0), 500 mM NaCl, 8 M urea, 5 mM imidazole, and 1 mM β-mercaptoethanol. The suspension was incubated with constant stirring for 2 h at 25 °C to facilitate complete solubilization of the rSTIP. The solubilized inclusion-body suspension was then centrifuged at 12,000 rpm for 20 min at 4 °C to remove insoluble material. The resulting supernatant was carefully collected and passed through a 0.22 µm syringe filter prior to subsequent refolding [27].

2.4.2. Refolding Strategy I: On-Column Refolding Using Ni-NTA Affinity Chromatography

The rSTIP fusion protein was purified by Ni-NTA affinity chromatography with simultaneous on-column refolding, following the method described by Mirhosseini et al. [28]. Briefly, 2 mL of Ni-NTA resin was packed into a gravity-flow column and equilibrated with the solubilization buffer. Following solubilization and filtration, the resulting protein solution was directly loaded onto the equilibrated Ni-NTA column. To enhance protein binding to the resin, the flow-through was reloaded onto the column, followed by incubation at room temperature for 1 h. On-column refolding was performed using Ni-NTA affinity chromatography. The resin was equilibrated with 3 column volumes of the solubilization buffer, followed by loading of 5 mL of the solubilized protein sample onto the column. The column was subsequently subjected to a linear urea gradient from 8 M to 0 M to facilitate gradual removal of the denaturant and on-column refolding of the bound protein. Following complete removal of urea, the column was washed with 3 column volumes of refolding buffer (20 mM Tris-HCl, pH 8.0, 500 mM NaCl, 20 mM imidazole, and 1 mM β-mercaptoethanol). The bound rSTIP was subsequently eluted using an imidazole gradient from 20 to 500 mM, and 2 mL fractions were collected for analysis of trypsin inhibitory activity. The eluted protein fractions were pooled and dialyzed against 20 mM Tris-HCl (pH 8.0) at 4 °C with multiple buffer exchanges to remove imidazole. The protein concentration was determined using the Bradford assay, and trypsin inhibitory activity was assessed using BApNA as the chromogenic substrate. The purified protein was stored at 4 °C until further analysis.

2.4.3. Refolding Strategy II: Glutathione-Mediated Dialysis

The solubilized rSTIP protein was subjected to dialysis against 50 mM Tris-HCl (pH 8.0) containing 0.4 M sucrose, 3 mM reduced glutathione (GSH), and 0.3 mM oxidized glutathione (GSSG) at 4 °C overnight, as described by Mirhosseini et al. [28]. The protein sample was subsequently dialyzed against 50 mM Tris-HCl (pH 8.0) for 2 h with two buffer exchanges to remove the refolding components. Following dialysis, the protein concentration was determined using the Bradford assay, and trypsin inhibitory activity was assessed using BApNA as the chromogenic substrate. Prior to the insecticidal assay, the refolded protein was further dialyzed against 50 mM Tris-HCl (pH 8.0) to remove residual components that could interfere with the assay.

2.5. Protein Concentration Determination

Protein concentration was determined using the Bradford assay, with bovine serum albumin (BSA) used as the standard. A series of BSA standards at concentrations of 31.25, 62.5, 125, 250, 500, and 1000 µg/mL were prepared to generate the standard curve. For the assay, 5 µL of the protein sample was mixed with 250 µL of Bradford reagent and incubated for 5 min at room temperature. Absorbance was measured at 595 nm using a microplate reader (Agilent BioTek, Santa Clara, CA, USA; Synergy H1). All measurements were performed in triplicate [29].

2.6. SDS-PAGE and Native PAGE Analysis

SDS-PAGE and Native PAGE were used to examine the electrophoretic profiles of purified recombinant STI-penetratin fusion protein (rSTIP). For SDS-PAGE, 10 µg of rSTIP was mixed with sample buffer containing 0.5 M Tris-HCl (pH 6.8), 10% SDS, 0.25% β-mercaptoethanol, 20% glycerol, and 0.5% bromophenol blue. The samples were heated at 95 °C for 5 min and subsequently separated on a 12% polyacrylamide gel. For Native PAGE, 10 µg rSTIP was prepared in a non-denaturing sample buffer containing 0.24 M Tris-HCl (pH 6.8), 30% glycerol, and 0.03% bromophenol blue before electrophoresis on a 7% polyacrylamide gel. Following electrophoresis, the gels were stained with Coomassie

Brilliant Blue R-250, and the protein bands were documented using a GelDoc imaging system (Bio-Rad Laboratories, Hercules, CA, USA).

2.7. Trypsin Inhibition Assay Using Nα-Benzoyl-DL-Arginine 4-Nitroanilide Hydrochloride (BApNA)

Trypsin inhibitory activity was determined using bovine pancreatic trypsin and the chromogenic substrate, Nα-Benzoyl-DL-arginine 4-nitroanilide hydrochloride (BApNA). Briefly, 30 µL of Soybean trypsin inhibitor (STI) or rSTIP fusion protein (300 µg/mL) was mixed separately with 30 µL of trypsin (300 µg/mL) in individual tubes. Subsequently, 100 mM Tris-HCl buffer (pH 8.0) containing 20 mM $CaCl_2$ was added to a final reaction volume of 300 µL, and the mixture was incubated at 37 °C for 15 min. Following pre-incubation, 500 µL of BApNA (1.25 mM) was added, and the reaction mixture was incubated at 37 °C for an additional 15 min. The reaction was terminated by adding 200 µL of 30% glacial acetic acid. Absorbance was measured at 410 nm using a microplate reader (BioTek Synergy H1). One trypsin inhibitor unit (TIU) was defined as the amount of inhibitor required to decrease the absorbance by 0.01 units at 410 nm under the specified assay conditions [30]. Trypsin inhibition was calculated from the reduction in absorbance relative to the uninhibited trypsin control using the following equation:

$$\% \text{ inhibition} = \frac{A_{\text{control}} - A_{\text{sample}}}{A_{\text{control}}} \times 100$$

where A_{control} is the absorbance of the reaction containing trypsin without an inhibitor, and A_{test} is the absorbance of the reaction containing STI or rSTIP. Absorbance values were blank corrected before calculation, wherever applicable. Relative inhibitory activity was expressed with native STI defined as 100%.

2.8. LC-MS/MS Analysis of rSTIP

2.8.1. In-Solution Digestion

Approximately 100 µg of purified rSTIP was resuspended in 20 µL of 25 mM ammonium bicarbonate (NH_4HCO_3) buffer (pH ~8.0). Disulfide bonds were reduced by adding freshly prepared dithiothreitol (DTT) to a final concentration of 10 mM, followed by incubation at 56 °C for 45 min. After incubation, the samples were briefly centrifuged and cooled to room temperature. Iodoacetamide, freshly prepared at a concentration of 250 mM in 25 mM ammonium bicarbonate buffer, was then added to a final concentration of 25 mM. The reaction mixture was then incubated in the dark for 30 min at room temperature to alkylate the reduced cysteine residues. For proteolytic digestion, 4 µL of sequencing-grade trypsin (0.5 mg/mL) was added at an enzyme-to-protein ratio of 1:50, and the reaction mixture was incubated overnight at 37 °C with gentle shaking. Following digestion, the samples were briefly centrifuged at 2000 rpm for 1 min, and the reaction was terminated by adding 2 µL of 5% formic acid (FA). The resulting peptide samples were dried to completion using a SpeedVac (Eppendorf SE, Hamburg, Germany) concentrator and reconstituted in 20 µL of the appropriate LC starting buffer prior to LC-MS/MS analysis [31].

2.8.2. LC-MS/MS Analysis

The resulting tryptic peptides were analyzed using a nanoACQUITY UPLC® system (Waters) coupled to a SYNAPT XS HDMS mass spectrometer (Waters). Peptide separation was performed using a trap column (nanoEase M/Z Symmetry® 180 µm × 20 mm, C18, 5 µm; Waters Corporation, Milford, MA, USA) and an analytical column (nanoEase M/Z Symmetry® 75 µm × 200 mm, C18 T3, 1.8 µm; Waters). The injection volume was 2.0 µL, and the flow rate was maintained at 300 nL/min. The mobile phase consisted of solvent A (0.1% formic acid in water) and solvent B (0.1% formic acid in acetonitrile).

Peptide separation was achieved using a gradient starting at 5% solvent B for 4 min, followed by a linear increase to 35% B, which was maintained until 49 min. The proportion of solvent B was subsequently increased to 85% at 54 min, followed by re-equilibration to 5% B for the remaining 13 min. The total chromatographic run time was 67 min. Data were acquired in positive electrospray ionization (ESI) mode using MassLynx 4.2 SCN 1028 software. The acquired raw mass spectral data were converted into Mascot generic format (mgf) files.

2.8.3. *De Novo* Peptide Sequencing Using PEAKS Studio and DeNovoGUI

The raw spectra were converted to mgf files, which were then used for *de novo* sequencing using PEAKS Studio (version 10.6, Bioinformatics Solutions Inc., Waterloo, ON, Canada) software. The search parameters were defined as follows: precursor ion mass tolerance of 10 ppm and fragment ion mass tolerance of 0.2 Da. Carbamidomethylation of cysteine residues was set as a fixed modification, whereas deamidation of asparagine and glutamine and oxidation of methionine were specified as variable modifications. Trypsin was designated as the proteolytic enzyme, allowing up to two missed cleavages. Database searches were performed against UniProt [32].

To further investigate the presence of the penetratin-derived sequence in the recombinant fusion protein, the mass spectra were further analysed using DeNovoGUI (version 1.16.8; Department of Bio and Health Informatics, Technical University of Denmark, Kongens Lyngby, Denmark), employing the Novor, DirecTag and PepNovo+ algorithms for *de novo* peptide sequencing. The resulting peptide sequences were manually examined for matches to the penetratin sequence.

2.9. Insecticidal Activity of Recombinant STI-Penetratin Fusion Protein

2.9.1. Preparation of Standard Food Medium

The standard Drosophila food medium was prepared per 100 mL using the following composition: corn flour (6 g), yeast (5 g), D-glucose (4 g), sucrose (3 g), yeast extract (1 g), agar (1 g), and malt extract (250 mg). The mixture was boiled until it was completely dissolved and subsequently autoclaved. After cooling to approximately 55 °C, 600 µL of propionic acid and 100 mg of benzoic acid (dissolved in 1 mL of 100% ethanol) were added as antifungal preservatives. The refolded fusion protein of concentrations 0.25 mg/mL, 0.5 mg/mL and 0.75 mg/mL was overlaid on top of the solid 1 mL food before the addition of larvae.

2.9.2. Preparation of Apple-Agar Plates for Larval Collection

Apple-agar plates were prepared by dissolving 3 g of agar in 100 mL of distilled water and 10 g of sucrose in 100 mL of apple juice. The two solutions were combined and maintained at 65 °C with continuous stirring for 30 min. After cooling to approximately 55 °C, 1.2 mL of propionic acid and 200 mg of benzoic acid (dissolved in 2 mL of 100% ethanol) were added. The prepared medium was poured into sterile Petri dishes, allowed to solidify, and stored at 4 °C until use [33]. Adult *Drosophila melanogaster* was transferred to cages containing apple-agar plates to induce oviposition. The plates were replaced every 8–10 h, and after 24 h, age-synchronized first-instar larvae were collected for subsequent toxicity assays [34].

2.9.3. Oral-Based Developmental Assay

Thirty first-instar larvae were transferred into individual vials overlaid with 300 µL of 50 mM Tris HCl as a control, rSTIP and STI with concentrations of 0.25 mg/mL, 0.5 mg/mL and 0.75 mg/mL. The vials were maintained at 25 °C until adult emergence. Mortality

was assessed by recording the number of larvae that failed to reach the pupal or adult stage [34,35]. Three independent vials were used for each concentration treatment, with each vial considered one biological replicate.

2.9.4. Contact-Based Assay

To evaluate the biological effects of the STI-penetratin fusion protein following topical exposure, a topical spray-based assay was employed. Unlike the developmental assay, where uptake may occur through feeding, this approach was designed to minimize feeding-mediated uptake and evaluate the biological effects of topical exposure. Thus, the assay enabled comparison of the responses to native STI and rSTIP following surface application, although direct penetration or tissue uptake of the fusion protein was not assessed.

10 synchronized second instar (L2) larvae of *D. melanogaster* were transferred onto a 35 mm Petri dish containing 5% agar. To prevent starvation without promoting feeding-based uptake, a rectangular piece of blotting paper soaked in 3% sucrose solution was carefully placed within the dish [36,37]. rSTIP and native STI were prepared at a concentration of 0.75 mg/mL, based on the concentration range evaluated in the developmental assay. The protein solution was applied using a 3 mL capacity glass spray bottle positioned approximately 10 cm away from the larvae. Two spray actuations delivered a combined volume of 250 µL per dish, distributed evenly over the assay setup. Applications were performed at 0 and 24 h. Control larvae were treated with 50 mM Tris-HCl buffer (pH 8.0) under identical conditions. Following treatment, the plates were incubated at 24 °C for 36 h, and larval responses were monitored to assess the effect of topical exposure. Three independent Petri dishes, each containing 10 larvae, were used per treatment, with each dish considered one biological replicate.

2.10. Statistical Analysis

All experiments were performed using three independent biological replicates, and data are presented as mean ± standard deviation (SD), where applicable. Statistical analyses and graphical representations were performed using R (version 4.6.1; R Foundation for Statistical Computing, Vienna, Austria). For the oral assay, pupation and adult emergence were analysed using binomial generalized linear models (GLMs), with treatment, concentration, and their interaction included as explanatory variables. Bias-reduced estimation was used to account for outcomes with very low or zero observed proportions. Comparisons with the untreated control were handled separately. For the topical assay, larval development and mortality were analysed using binomial GLM. Each vial in the oral assay and each Petri dish in the topical assay was considered one independent experimental replicate. A *p*-value of less than 0.05 was considered statistically significant.

3. Results

3.1. Sequence Validation of the Recombinant STI-Penetratin Construct

The nucleotide sequence of the recombinant STI-penetratin construct was verified by Sanger sequencing prior to protein expression. The designed construct comprised 689 bp and encoded the expected STI-penetratin fusion protein containing the N-terminal His_6 tag, TEV recognition sequence, soybean trypsin inhibitor, flexible G_8 linker, and C-terminal penetratin moiety (Figure 1). Sanger sequencing was performed using forward and reverse primers, and the obtained sequences were aligned with the reference construct sequence. Both forward and reverse sequencing reads showed 100% sequence identity with the corresponding reference sequence, with no mismatches or gaps detected in the aligned regions. The reverse sequencing read covered the complete 689 bp construct, further confirming the integrity of the cloned sequence. Translation of the verified nucleotide

sequence yielded the expected recombinant protein sequence. The corresponding sequence alignment and BLAST analysis are provided in Supplementary Figure S1.



Figure 1. Schematic design of the recombinant soybean trypsin inhibitor-penetratin fusion protein. The recombinant STI-penetratin fusion construct comprises an N-terminal His_6-tag for affinity purification, a TEV protease cleavage site, the mature soybean trypsin inhibitor (STI), an eight-glycine (G_8) flexible linker, and the C-terminal cell-penetrating peptide penetratin. The G_8 linker provides flexibility and spatial separation between STI and penetratin, while penetratin was incorporated as the cell-penetrating peptide moiety of the fusion protein.

3.2. Expression and Recovery of Recombinant STI-Penetratin Fusion Protein

The rSTIP fusion protein was expressed in *E. coli* BL21(DE3) following induction with IPTG. The recombinant protein was predominantly recovered in the insoluble fraction, indicating formation of inclusion bodies. The inclusion bodies were subsequently solubilized under denaturing conditions and subjected to Ni-NTA affinity chromatography for purification and on-column refolding. The predicted molecular mass of the recombinant fusion protein was 25.18 kDa, and the construct was predicted to contain two disulfide bonds.

Expression of the recombinant STI-penetratin fusion protein was evaluated under different induction conditions by varying the IPTG concentration and incubation temperature. The recombinant protein was induced with 1 mM IPTG at 37 °C, 0.5 mM IPTG at 25 °C, and 0.5 mM IPTG at 16 °C, with an induction period of 8 h in each condition. Among the conditions examined, induction at 16 °C with 0.5 mM IPTG resulted in the most favourable expression profile and was therefore selected for subsequent protein production. SDS-PAGE analysis under the selected conditions revealed a distinct protein band of approximately 25 kDa predominantly in the insoluble fraction, whereas no corresponding band was detected in the soluble fraction (Figure 2A), indicating that the recombinant protein accumulated mainly as inclusion bodies. The isolated inclusion bodies were subsequently subjected to denaturation using 8 M urea. Following solubilization, SDS-PAGE analysis demonstrated substantial transfer of the recombinant protein into the soluble fraction, with only a small proportion remaining in the insoluble pellet (Figure 2B). The soluble protein migrated at approximately 25 kDa, consistent with the predicted molecular mass of the STI-penetratin fusion protein. A comparative SDS-PAGE analysis of the purified rSTIP and native STI showed distinct bands at approximately 25 kDa and 20 kDa, respectively (Figure 2D). The difference in apparent molecular mass was consistent with the predicted molecular mass of the recombinant fusion protein. Native PAGE analysis of refolded rSTIP revealed a prominent protein band approximately at 25 kDa (Supplementary Figure S2). The absence of distinct high-molecular-mass bands suggests protein aggregation was not present under the conditions examined.

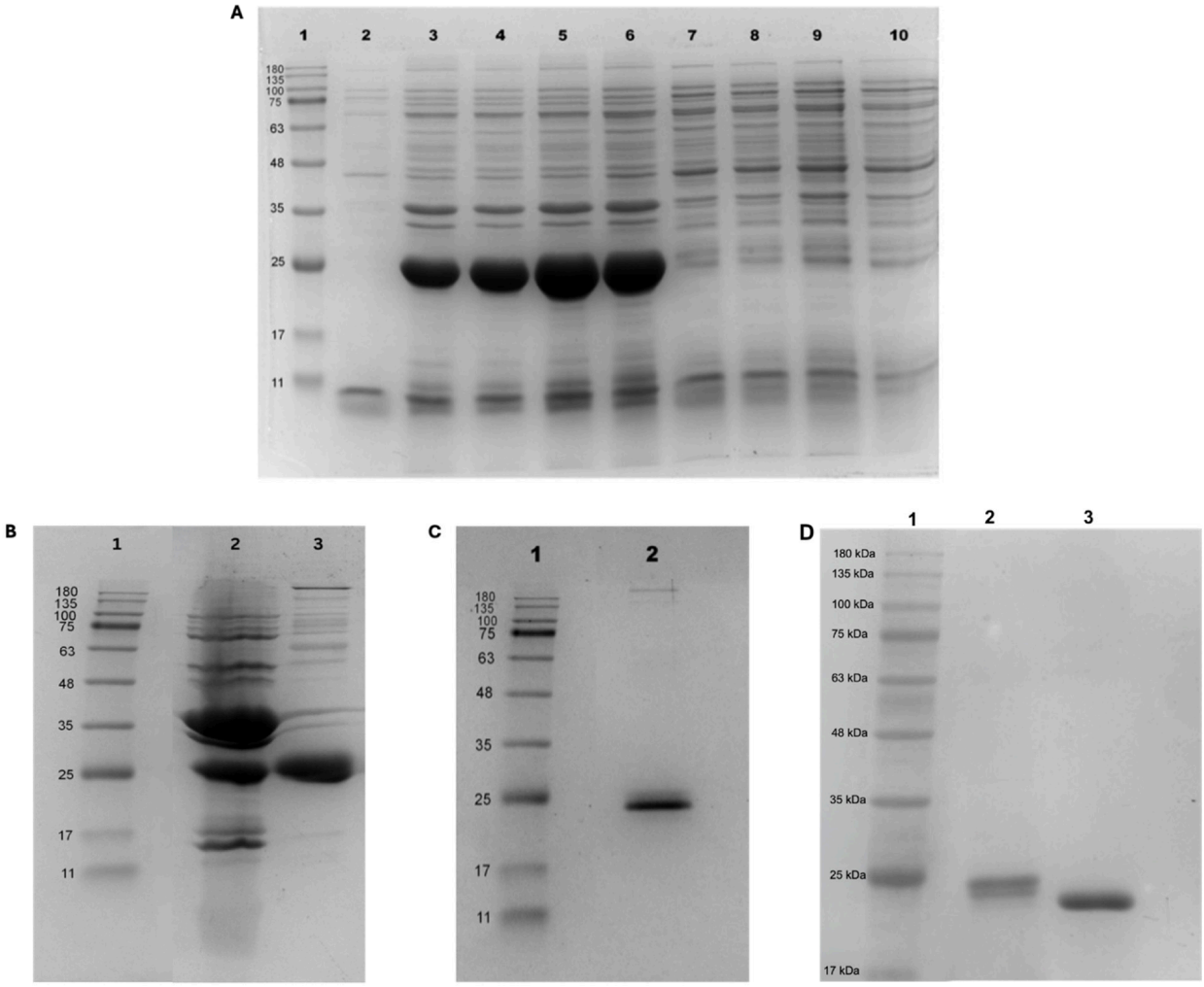


Figure 2. Expression, solubilization, and on-column purification of recombinant STI-penetratin fusion protein (rSTIP). (**A**) SDS-PAGE analysis of rSTIP expression following induction with 0.5 mM IPTG at 16 °C. Lane 1, molecular weight marker (11–180 kDa); Lane 2, uninduced cell lysate; Lanes 3–6, insoluble fractions collected at 6, 8, 10, and 12 h post-induction, respectively; Lanes 7–10, corresponding soluble fractions collected at 6, 8, 10, and 12 h post-induction, respectively. (**B**) SDS-PAGE analysis of rSTIP following solubilization of the inclusion bodies. Lane 1, molecular weight marker; Lane 2, insoluble fraction remaining after solubilization; Lane 3, soluble fraction containing the recombinant fusion protein at approximately 25 kDa. (**C**) SDS-PAGE analysis of rSTIP following on-column refolding and Ni-NTA affinity purification. Lane 1, molecular weight marker; Lane 2, protein fraction after Ni-NTA purification. (**D**) SDS-PAGE analysis of the purified rSTIP and native STI. Lane 1, molecular weight marker; Lane 2, rSTIP and Lane 3, native STI.

3.3. Refolding and Purification of Recombinant STI-Penetratin Fusion Protein

3.3.1. Ni-NTA-Based On-Column Refolding and Purification

The solubilized rSTIP protein was subjected to Ni-NTA affinity chromatography with on-column refolding through a gradual reduction in the urea concentration. SDS-PAGE analysis of the eluted fractions showed substantial enrichment of the recombinant protein, with a marked reduction in non-specific protein bands following purification (Figure 2C). The purified protein was recovered at a concentration of 0.3 mg/mL, as determined by the Bradford assay. Functional analysis using the BApNA-based trypsin inhibition assay showed that the protein exhibited a relative trypsin-inhibitory activity of 11.0 ± 1.55% ($n = 3$). Following dialysis against 20 mM Tris-HCl (pH 8.0), the inhibitory activity increased to 17.0 ± 2.1% ($n = 3$). The increase in activity following dialysis indicated improved recovery

of the functional state of the fusion protein following removal of imidazole and residual denaturants. The dialyzed protein was subsequently lyophilized and stored at 4 °C for further analysis.

3.3.2. Glutathione-Assisted Refolding

The solubilized inclusion-body fraction was subjected to refolding by dialysis against 50 mM Tris-HCl (pH 8.0) supplemented with 0.4 M sucrose, 3 mM GSH, and 0.3 mM GSSG at 4 °C overnight. Following this initial glutathione-assisted refolding step, the protein was dialyzed against 50 mM Tris-HCl (pH 8.0) for 2 h with two buffer changes. The protein concentration after the initial refolding step was 935 µg/mL, which decreased to 860 µg/mL following the final dialysis against Tris-HCl buffer, as determined by the Bradford assay. The functional activity of the refolded rSTIP was assessed using the BApNA-based trypsin inhibition assay. The protein exhibited a relative trypsin-inhibitory activity of 46.0 ± 1.8% immediately after refolding and 65.5 ± 1.88% following the final dialysis ($n = 3$ for each condition; Figure 3). Native STI, used as the reference, exhibited 100% inhibitory activity under the assay conditions. The increase in inhibitory activity following the final dialysis may be attributed to further conformational stabilization of the refolded protein during buffer exchange, along with removal of residual GSH/GSSG and other small refolding components that were present after the initial refolding step. The dialyzed, glutathione-refolded fusion protein was further purified by Ni-NTA affinity chromatography and eluted using an imidazole gradient from 50 to 500 mM. The purified protein was subsequently dialyzed against 50 mM Tris-HCl (pH 8.0) before functional and insecticidal assays. The purification profile was consistent with the enrichment observed in the corresponding chromatographic fractions shown in Figure 2C.

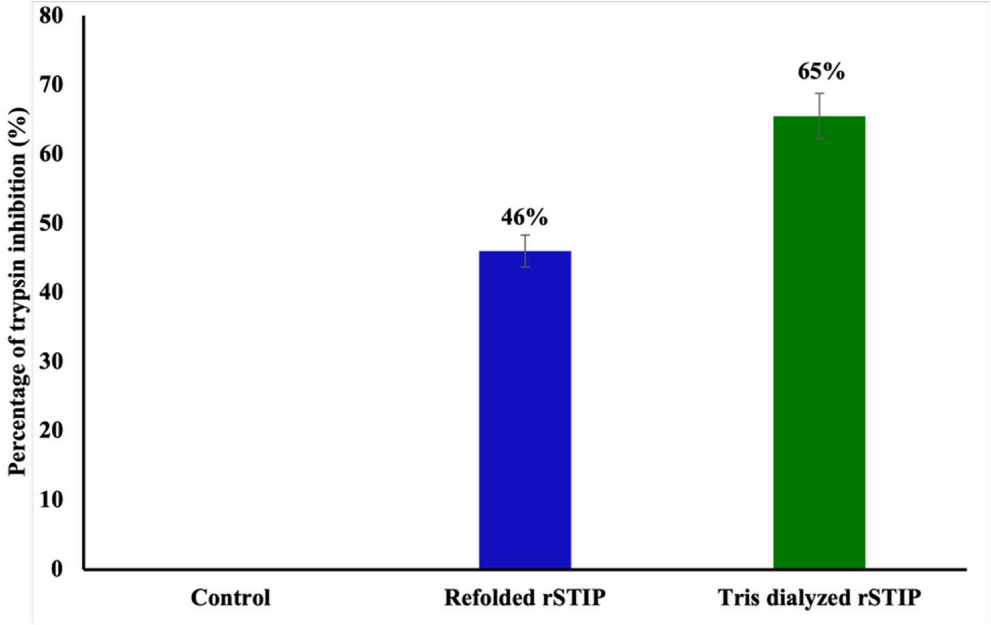


Figure 3. Trypsin inhibitory activity of refolded rSTIP before and after dialysis. The plot illustrates the trypsin inhibitory activity of the refolded rSTIP, which exhibited 46% inhibition before dialysis and increased to 65.5% following dialysis against Tris-HCl buffer.

3.4. LC-MS/MS Characterization of Recombinant Protein

The purified recombinant protein was subjected to tryptic digestion and analyzed by LC-MS/MS to confirm its molecular identity. Database-assisted analysis using PEAKS Studio identified the protein as soybean trypsin inhibitor from *Glycine max*, corresponding

to UniProt accession P01070. The identified peptides showed correspondence with the reference STI sequence, supporting the identity of the recombinant protein. To further validate the peptide assignments and obtain sequence information independent of database matching, de novo sequencing was performed using the MS/MS spectra. The resulting de novo-derived peptide sequences were compared with the reference STI sequence, and several peptides showed clear alignment with the corresponding regions of STI (Table 1).

Table 1. *De novo*-derived peptide sequences of soybean trypsin inhibitor (STI) identified by LC-MS/MS analysis. *De novo*-derived peptide sequences corresponding to soybean trypsin inhibitor (STI) identified by LC-MS/MS analysis. The table presents the peptide sequences, charge states, and corresponding *m*/*z* values obtained from the MS/MS spectra.

Number	Identified Peptide Sequence	Charge State	*m*/*z*
1	NKPLVVQFQKLDK	3	519.6451
2	NKPLVVQFQK	2	400.9109
3	VSDDEFNNYK	2	615.7698
4	CPLTVVQSR	3	530.2864
5	NELDKGIGTIISSPYR	3	588.3162
6	AAPTGNER	2	408.2061
7	IRFAEGHPLSLK	2	740.9351
8	GIGTIISSPYR	2	582.3243

The presence of penetratin moiety was investigated by reanalysing the MS/MS data using the DeNovoGUI software suite (version 1.16.8) where Novor, DirectTag and PepNovo+ peptide sequencing algorithms were employed. This analysis yielded a short peptide sequence, WFQN, that corresponds to the sequence of penetratin. The corresponding MS/MS spectrum is provided in Supplementary Figure S3. This finding provides preliminary peptide-level evidence for a sequence corresponding to part of the penetratin moiety.

3.5. Developmental Toxicity Following Dietary Exposure

The insecticidal activity of recombinant protein was assessed in *Drosophila melanogaster* larvae using a developmental assay following dietary exposure, and its effects were compared with those of native STI and the untreated control. Exposure to both rSTIP and native STI impaired larval development, as evidenced by concentration-dependent reductions in pupation and adult emergence, with rSTIP producing a more pronounced effect than native STI compared with the control (Figure 4). In the control group, 83% of larvae progressed to the pupal stage, and 76% developed into adults. In contrast, pupation in the rSTIP-treated groups decreased to 33%, 17%, and 0% at 0.25, 0.5, and 0.75 mg/mL, respectively. Adult emergence showed a similar pattern, declining to 16%, 10%, and 0% at the corresponding concentrations. Native STI also impaired development, but the effect was comparatively less pronounced, with pupation rates of 50%, 26%, and 13% and adult emergence rates of 50%, 26%, and 13% at 0.25, 0.5, and 0.75 mg/mL, respectively. Thus, dietary exposure to rSTIP produced a stronger developmental effect than native STI, with complete suppression of pupation and adult emergence observed at 0.75 mg/mL.

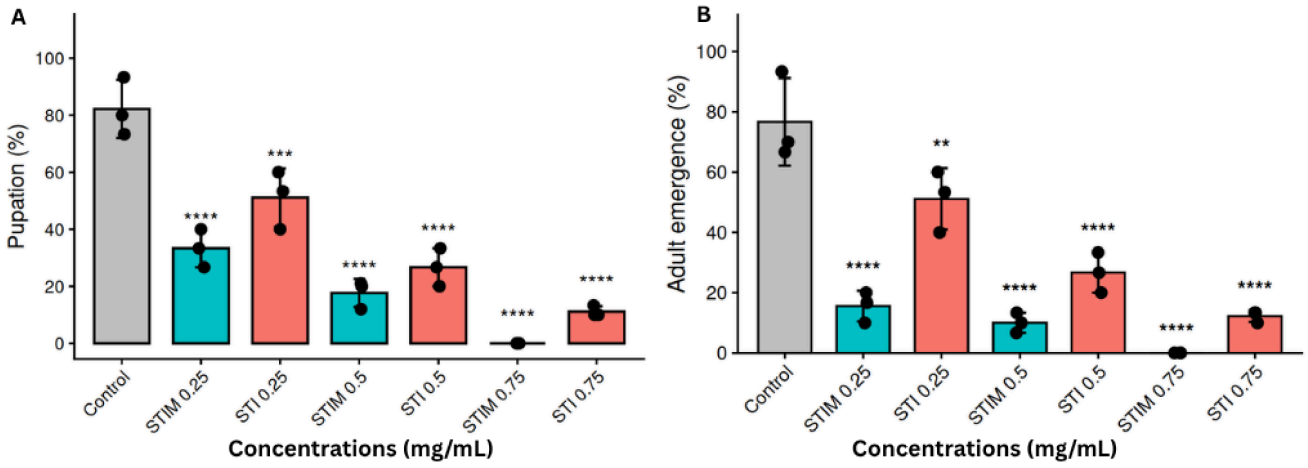


Figure 4. Effect of rSTIP and STI on larval development of *Drosophila melanogaster*. (**A**) Percentage of larvae progressing to the pupal stage following dietary exposure to different concentrations of rSTIP and native STI. (**B**) Percentage of adult emergence following exposure to rSTIP and STI. Grey bars represent the control, teal bars represent rSTIP, and coral bars represent native STI. Data are presented as mean ± standard deviation (SD) from three independent experiments. Developmental outcomes were analysed using binomial generalized linear models (GLMs). Statistical comparisons between rSTIP- and STI-treated groups at corresponding concentrations were performed as appropriate. Asterisks indicate statistically significant differences: $p < 0.01$ (**), $p < 0.001$ (***), and $p < 0.0001$ (****). Each dot indicates each replicate value. The experiment was performed in biological triplicates.

3.6. Topical Efficacy of rSTIP

The topical activity of recombinant rSTIP was subsequently evaluated to compare the biological effects of rSTIP and native STI following surface application. The developmental responses of the larvae were monitored for 36 h following topical treatment. During this observation period, the control larvae continued to progress through normal developmental stages, with two of ten larvae reaching the pupal stage and the remaining eight larvae progressing to the late third-instar (L3) stage. In contrast, larvae treated with native STI exhibited delayed developmental progression, with only two larvae reaching the L3 stage, while the remaining eight larvae remained at the second-instar (L2) stage. Notably, treatment with rSTIP resulted in complete lethality, with all ten larvae found dead within the 36 h observation period (Figure 5). Developmental progression and mortality were evaluated as distinct endpoints: developmental progression was assessed based on the larval stage reached or pupation, whereas mortality was recorded separately based on the number of dead larvae. As the observation period was limited to 36 h, the developmental progression observed in the control and STI-treated groups represents the stage reached within this experimental window rather than the final developmental outcome. Nevertheless, compared with the control, native STI clearly delayed larval progression, whereas rSTIP produced a pronounced lethal effect within the same period. Thus, under the topical exposure conditions, rSTIP caused a markedly stronger biological effect than native STI, which primarily manifested as developmental retardation. The enhanced response observed with rSTIP is consistent with a possible contribution of the penetratin moiety; however, the mechanism underlying this difference was not directly investigated in the present study.

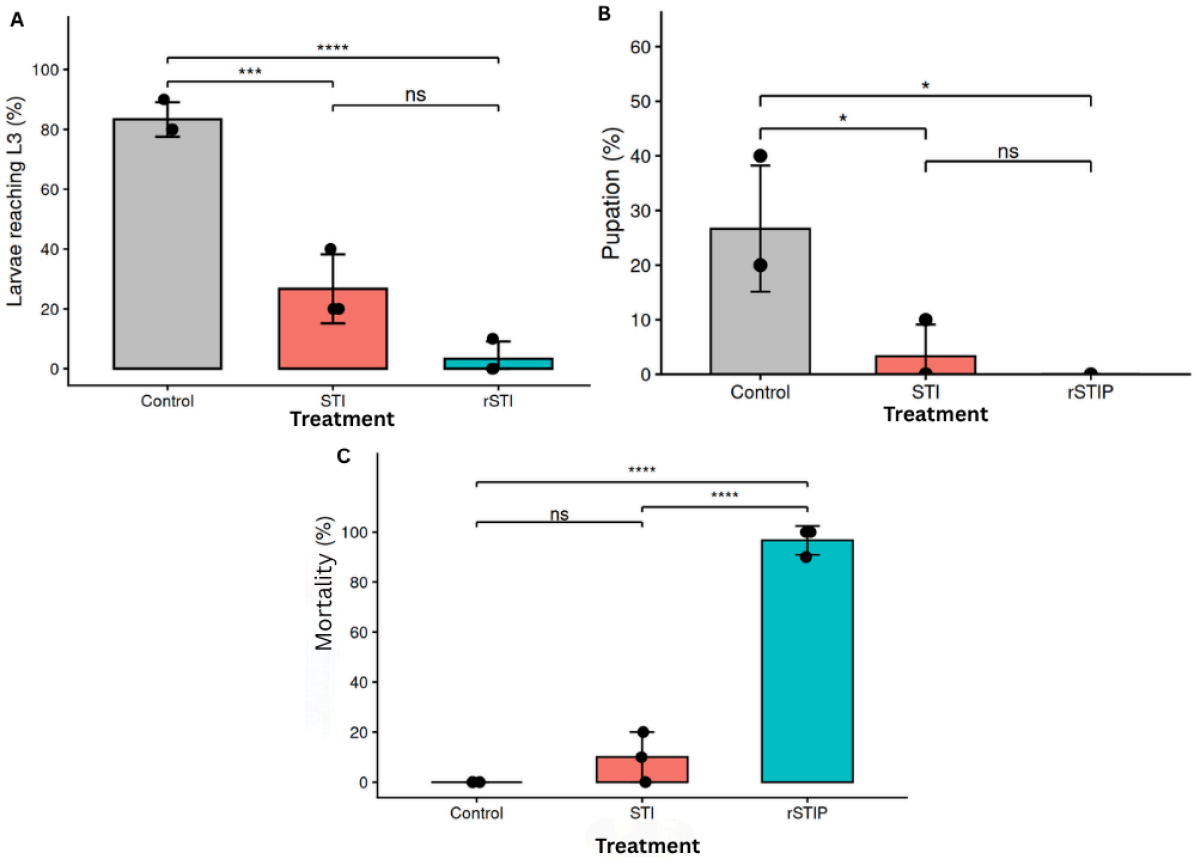


Figure 5. Effect of topical application of native STI and rSTIP (0.75 mg/mL) on the developmental progression and mortality of *Drosophila melanogaster* larvae after 36 h of treatment. (**A**) Percentage of larvae remaining at the L3 stage. (**B**) Percentage of larvae progressing to the pupal stage. (**C**) Percentage of larval mortality following topical treatment. Grey bars represent the control, teal bars represent rSTIP, and coral bars represent native STI. Data are presented as mean ± standard deviation (SD) from three independent replicates. Each Petri dish was considered an independent experimental replicate. Statistical differences were analysed using binomial generalized linear models, with appropriate pairwise comparisons between treatments. Asterisks indicate statistically significant differences: $p < 0.05$ (*), $p < 0.001$ (***), and $p < 0.0001$ (****); ns, not significant. Each dot represents each replicate value. The experiment was performed in biological triplicates.

4. Discussion

Soybean trypsin inhibitor (STI) is a well-characterised plant defense protein with established activity against trypsin and a documented role in insect growth and development. The native STI molecule comprises 181 amino acid residues stabilized by two disulfide bonds, and its inhibitory activity arises from the formation of a stable complex with trypsin through interactions involving its reactive-site loop [38]. Studies have demonstrated the potential of STI as an insect defense protein, where dietary exposure with STI to insects has been reported to reduce larval survival and pupation [12,39]. Although STI has demonstrated insecticidal activity following oral exposure [40,41], its effectiveness may be influenced by the route through which the protein reaches and interacts with the insect [42,43]. Therefore, in the present study, penetratin, a cell-penetrating peptide (CPP), was incorporated with STI to investigate whether CPP fusion could alter the insecticidal activity of STI following oral and topical exposure. Accordingly, a recombinant soybean trypsin inhibitor (rSTIP) fusion construct was successfully generated, and its nucleotide sequence was confirmed by Sanger sequencing. The corresponding recombinant protein was subsequently expressed, purified, and characterized for its molecular and functional properties.

The expressed recombinant fusion protein was predominantly recovered in the insoluble fraction, indicating its accumulation as inclusion bodies. The formation of inclusion bodies during recombinant protein expression in *E. coli* is influenced by multiple factors, including high expression rates that exceed the cellular folding capacity, limitations in the host protein-folding machinery, the requirement for disulfide-bond formation, and the intrinsic physicochemical properties of the target protein. Improper or incomplete folding can expose hydrophobic residues that are normally buried within the native protein structure, promoting intermolecular hydrophobic interactions and subsequent aggregation into inclusion bodies [44–46]. The predominant accumulation of rSTIP in the insoluble fraction is consistent with previous reports describing recombinant soybean Kunitz trypsin inhibitor as an inclusion-body-associated protein when expressed in *E. coli* [47,48]. This pattern of insoluble protein accumulation may be attributed, at least in part, to the structural requirements of STI for correct disulfide-bond formation. Mature STI contains two disulfide bonds, whereas the reducing environment of the *E. coli* cytoplasm is unfavourable for efficient formation of native disulfide linkages, potentially limiting proper folding of the recombinant protein [47,49]. As rSTIP was predominantly recovered as inclusion bodies, solubilization was necessary to disrupt the aggregated protein structures and release the recombinant protein into a denatured, soluble state. However, solubilization alone does not restore the native conformation required for trypsin inhibitory activity. Therefore, a subsequent refolding step was necessary to allow the solubilized protein to regain its appropriate three-dimensional structure and disulfide-bond arrangement, thereby enabling recovery of its trypsin inhibitory activity.

The efficiency of protein refolding is strongly dependent on the conditions used to restore the native conformation of the target protein, particularly for disulfide-containing proteins in which appropriate disulfide-bond formation and rearrangement are essential for functional recovery. In the present study, two refolding strategies were evaluated for the recovery of functional rSTIP: on-column refolding using Ni-NTA chromatography and glutathione-assisted refolding by dialysis. The on-column refolding approach resulted in 11% trypsin inhibitory activity following elution, which increased to 17% after subsequent dialysis against Tris-HCl buffer. In comparison, glutathione-assisted refolding resulted in 46% inhibitory activity following the initial refolding step, with activity increasing further to 65.5% after subsequent dialysis. The partial recovery of inhibitory activity observed following glutathione-assisted refolding may be associated with the redox environment provided by the GSH/GSSG. For disulfide-containing proteins, an appropriate balance between reduced and oxidized thiol species can facilitate the formation and reshuffling of disulfide bonds during refolding, thereby promoting attainment of the native conformation [50]. Multiple studies have demonstrated the importance of glutathione-mediated redox conditions in oxidative protein folding and have shown that GSH/GSSG systems can support disulfide bond formation and rearrangement during protein refolding [51–53]. In comparison with the glutathione-assisted refolding, on-column refolding resulted in 17% trypsin inhibitory activity following dialysis against Tris-HCl buffer. This strategy was expected to allow the denatured protein to remain immobilized on the Ni-NTA matrix during removal of the denaturant, which can limit intermolecular interactions and reduce aggregation during the early stages of refolding [54].

However, efficient refolding on an affinity matrix requires a balance between maintaining sufficient interaction of the His-tagged protein with the resin and permitting progressive conformational rearrangement as the denaturant concentration decreases. Previous studies have shown that the efficiency of on-column refolding can be influenced by protein loading, flow rate and the concentration of residual denaturant, with inadequate spatial separation of protein molecules on the matrix potentially promoting aggregation of incompletely re-

folded intermediates [53,55]. Despite the potential advantage of immobilization in reducing intermolecular aggregation, the on-column conditions employed in the present study may not have provided a sufficiently favorable environment for complete refolding of rSTIP into its active conformation. Thus, although on-column refolding permitted recovery of active rSTIP, it was less effective under the conditions employed in this study than the glutathione-assisted dialysis approach.

Solubilization of the inclusion bodies followed by the washing step helped to remove the associated membrane proteins, thereby reducing the protein impurities present in the solubilized fraction (Figure 2B). The resulting fraction was subsequently subjected to Ni-NTA affinity chromatography, enabling enrichment of the recombinant His_6-tagged rSTIP. Because the N-terminal His_6 tag was retained in the recombinant construct during purification and subsequent biochemical and insecticidal characterization, its potential influence on the properties of the recombinant protein should also be considered. Although polyhistidine tags are generally considered to have minimal effects on the native structure of recombinant proteins, their influence on protein stability and functional properties can be protein-dependent [56]. Very few studies have demonstrated that the presence of an N-terminal polyhistidine tag can alter protein thermal stability and, in some cases, can influence reproducibility of experiments [57,58]. Therefore, although the present study does not provide evidence that the His_6 tag altered the activity of rSTIP, a potential contribution of the tag to the observed biochemical or biological properties cannot be completely excluded.

The molecular identity of the purified recombinant protein was subsequently evaluated by LC-MS/MS. The mass spectrometric data provided sequence-level evidence for the STI component of the recombinant protein. During the analysis, eight de novo derived peptides covering 68 amino acid residues of the 181-residue STI reference sequence were identified. SDS-PAGE analysis showed an apparent molecular mass of approximately 25 kDa for rSTIP, compared with approximately 20 kDa for native STI, consistent with the expected increase in molecular mass associated with the fusion construct (Figure 2D). Since penetratin contains multiple lysine and arginine residues, tryptic digestion leads to the generation of short peptide fragments that are less amenable to confident MS/MS identification. Still, reanalysis of the MS/MS data using DeNovoGUI software tool (version 1.16.8) identified a short peptide sequence, WFQN, corresponding to the residues in the 6–9 position of the penetratin sequence, RQIKIWFQNRRMKWKK (Supplementary Figure S3). Thus, the present LC-MS/MS analysis confirms the STI component but does not constitute complete sequence-level validation of the full-length STI-penetratin fusion protein. Alternative proteases, such as chymotrypsin or V8 protease, with different cleavage specificities, could provide complementary peptide coverage in future analyses [59]. Importantly, the entire nucleotide sequence of the STI-penetratin fusion construct could be verified through Sanger sequencing. The SDS-PAGE profile, identification of STI-derived peptides, detection of the WFQN sequence corresponding to part of penetratin, and confirmation of the gene construct together support the identity of rSTIP. However, definitive protein-level confirmation of the complete penetratin moiety remains to be established.

In addition to the SDS-PAGE analysis, Native PAGE was performed to examine the migration profile of refolded rSTIP under non-denaturing conditions (Supplementary Figure S2). The gel revealed a prominent band of rSTIP. There was no distinct high-molecular-mass species observed, suggesting no aggregation under the conditions tested. However, Native PAGE alone is insufficient to establish the oligomeric state of rSTIP or exclude the presence of soluble aggregates. Therefore, potential protein heterogeneity should be considered when interpreting the biochemical and insecticidal properties of the refolded protein. Further analysis using size-exclusion chromatography or another complementary technique would be required to establish its oligomeric state and assess its homogeneity.

The oral exposure experiments demonstrated that native STI exerted a developmental effect on *D. melanogaster* larvae. This observation is consistent with earlier reports showing that dietary soybean trypsin inhibitor can adversely affect insect growth and development, including reduced larval survival and pupation and prolonged developmental duration in *Helicoverpa armigera* [12]. Similar effects have been reported for other plant-derived Kunitz-type protease inhibitors, where inhibition of digestive proteolysis was associated with reduced growth and delayed larval development [60]. Thus, rSTIP produced a stronger developmental response than native STI under the conditions tested, despite only partial recovery of trypsin inhibitory activity following refolding and dialysis.

Notably, rSTIP retained approximately 65.5% of the trypsin-inhibitory activity following refolding and dialysis. However, it is important to note that the insecticidal assays using the two protein preparations at equivalent mass concentrations need not represent equivalent trypsin-inhibitory activities. In addition to differences in measured trypsin-inhibitory activity, protein conformation, structural stability, and interactions with components of the insect gut may influence biological activity. Further studies using activity-normalized protein concentrations and detailed structural analyses are required to determine the contribution of these factors to the insecticidal effects of rSTIP. This finding suggests that the biological activity of rSTIP may not be determined solely by the measured inhibitory activity of the STI domain. Notably, rSTIP exhibited a stronger insecticidal response than native STI despite recovering only 65.5% of the trypsin-inhibitory activity of native STI following refolding and dialysis. This difference suggests that factors beyond intrinsic trypsin-inhibitory activity may contribute to the observed insecticidal effect. One possible explanation is that the incorporation of penetratin may have altered the biological accessibility of the STI component to susceptible insect tissues. With respect to the hypothesis, previous studies have reported that CPP fusion can enhance protein uptake in insects, including increased internalization and transepithelial transport of TAT-eGFP in *Bombyx mori* [61]. Similarly, the fusion of CPP-1838, a cell-penetrating peptide, to a spider venom-derived neurotoxin enhanced its contact aphidicidal activity and was associated with increased detection of the recombinant protein within aphid tissues following topical exposure [42]. These findings provide a rationale for considering enhanced protein delivery as a possible explanation for the observed activity of rSTIP. However, whether penetratin enhanced rSTIP delivery in the present study remains uncertain because protein uptake and tissue localization were not directly assessed. Furthermore, the absence of a free penetratin control prevents the specific contribution of penetratin from being distinguished from other effects of the fusion construct. Although enhanced accessibility to target proteases may contribute to the insecticidal response, this mechanism remains to be experimentally verified.

The topical exposure experiments further demonstrated a marked difference in the biological effects of native STI and rSTIP. While native STI primarily caused developmental retardation, rSTIP resulted in complete larval mortality within the 36 h observation period under the same exposure conditions. However, as rSTIP was evaluated at a single concentration (0.75 mg/mL), its concentration-dependent effects could not be established, and further studies using multiple concentrations are required to characterize its dose–response relationship. Despite this limitation, this finding is particularly notable because the insecticidal activity of STI has been predominantly associated with dietary exposure and inhibition of digestive proteases. Earlier studies have demonstrated that dietary administration of soybean trypsin inhibitor can reduce larval survival, retard growth, prolong post-embryonic development, and decrease pupation in *Helicoverpa armigera* [12]. Thus, the complete mortality observed following topical application demonstrates that the rSTIP fusion protein retained biological activity following surface exposure and produced a pronounced lethal effect under the conditions tested. The enhanced topical activity of

rSTIP is consistent with previous works showing that fusion of insecticidal proteins with delivery-enhancing components can improve their efficacy following surface application. For example, a study by Sukiran et al. reported that fusion of the spider venom peptide HxTx-Hv1h with snowdrop lectin significantly increased contact mortality against pea aphids compared with the unfused toxin. Fluorescence microscopy and immunoblotting also demonstrated greater persistence of the fusion protein after topical application, suggesting that improved delivery and retention contributed to its enhanced activity [62]. The relevance of a cell-penetrating peptide-based approach is further supported by studies demonstrating that CPPs can facilitate protein delivery in insect systems. In particular, penetratin has been shown to mediate *in vivo* delivery of a fused protein into insect tissues [63,64]. Beyond their roles in digestive physiology, serine proteases also participate in insect immune responses and other protease-dependent physiological processes in the hemolymph [13]. If rSTIP crosses the insect cuticle and reaches the hemocoel, it could potentially interfere with systemic protease activity and thereby contribute to the observed insecticidal effect. However, cuticular penetration and cellular uptake are distinct processes, and neither was directly investigated in the present study. Therefore, the greater biological effect observed with rSTIP following topical exposure is consistent with the possibility that incorporation of penetratin altered the accessibility or biological behaviour of the fusion protein. However, whether this difference resulted specifically from penetratin-mediated delivery cannot be determined from the present experiments because direct uptake was not assessed and a free penetratin control was not included.

Despite the biological activity observed for the recombinant STI-penetratin fusion protein, several limitations should be considered when interpreting the present findings. First, a free penetratin peptide control was not included at an equimolar concentration in the oral or topical bioassays primarily because the rSTIP construct was designed and synthesized as a single fusion gene containing the STI and penetratin sequences, rather than by separately producing the two components and fusing them through chemical strategies. Consequently, recombinant STI without penetratin and penetratin alone were not included as controls in the original experimental design. Consequently, the present experiments cannot distinguish whether the greater activity of rSTIP relative to native STI resulted from penetratin-mediated delivery, an independent biological effect of the penetratin moiety, or altered properties of the fusion protein. Further, though the topical exposure assay was designed to minimize feeding-mediated uptake, direct penetration through the larval surface, cellular internalization, tissue distribution, and persistence of rSTIP were not assessed. Therefore, the present study cannot establish whether the greater insecticidal activity observed following topical exposure resulted from enhanced penetration or cellular delivery of rSTIP. Direct localization approaches, such as fluorescence labelling of rSTIP or immunodetection in insect tissues, would be required to determine its penetration, cellular uptake, tissue distribution, and persistence. Thus, penetratin-mediated enhancement of protein delivery remains a possible mechanistic explanation rather than a directly demonstrated process. The insecticidal activity was evaluated exclusively in *D. melanogaster*, which limits the extrapolation of the findings to agriculturally relevant pest species. The recombinant construct retained the N-terminal His_6 tag during biochemical characterization and insecticidal assays. Although polyhistidine tags are generally considered to have minimal effects on many recombinant proteins, their effects can be protein-dependent. Therefore, a potential contribution of the affinity tag to the observed biochemical or biological properties of rSTIP cannot be completely excluded.

Furthermore, LC-MS/MS analysis provided sequence-level confirmation of the STI component but did not provide complete sequence coverage of the STI-penetratin fusion protein, particularly for the penetratin moiety. The absence of complementary protease-

based analysis therefore represents a limitation in the molecular characterization of the recombinant construct. In addition, the oligomeric state and aggregation profile of the refolded rSTIP were not quantitatively assessed even though Native PAGE indicates an absence of protein oligomerization. Taken together, these limitations indicate that although rSTIP exhibited greater insecticidal activity than native STI under the conditions tested, the specific contribution of penetratin to this activity and its underlying mechanism require further experimental validation. Additionally, the efficacy of rSTIP against agriculturally relevant insect pests, particularly those with distinct digestive protease profiles, remains to be established before its potential application in crop protection can be assessed.

The environmental stability and persistence of rSTIP in the field are also to be established. Nevertheless, the present study evaluated the biochemical and insecticidal activities of rSTIP under controlled laboratory conditions. Future studies should further investigate the stability of rSTIP under field-relevant environmental conditions and evaluate suitable formulation strategies to improve its protection against environmental degradation. Such investigations are necessary before it can have practical efficacy and suitability for agricultural pest management.

5. Conclusions

The present study describes the production and functional analysis of a recombinant soybean trypsin inhibitor-penetratin fusion protein (rSTIP) as well as its insecticidal activity against *Drosophila melanogaster*. Glutathione-assisted refolding yielded rSTIP with substantially higher trypsin inhibitory activity than on-column refolding, reaching 65.5% of the activity. LC-MS/MS analysis provided sequence-level confirmation of the recombinant protein. The insecticidal activity of rSTIP was higher than that of the native STI in oral and topical exposure assays, with topical application resulting in complete larval mortality within the 36 h observation period. Although the observed difference may be associated with altered biological properties of the STI-penetratin fusion construct, the absence of a free penetratin control and direct uptake measurements prevents attribution of the enhanced activity specifically to penetratin-mediated delivery. Further, the insecticidal activity of rSTIP observed against *D. melanogaster* should be considered preliminary and cannot be directly extrapolated to agricultural pest management. Detailed studies using agriculturally relevant insect pests with distinct digestive protease profiles are required to validate the insecticidal efficacy of rSTIP and establish its potential application as a protein-based insecticidal agent.

Supplementary Materials: The following supporting information can be downloaded at: https://www.mdpi.com/article/10.3390/agrochemicals5040049/s1, Figure S1: Sanger sequencing and BLAST analysis of the recombinant STI–penetratin construct; Figure S2: Native PAGE analysis of refolded recombinant STI–penetratin fusion protein (rSTIP); Figure S3: MS/MS spectrum corresponding to the peptide sequence WFQN, identified through DeNovoGUI-assisted de novo sequencing.

Author Contributions: S.S.: Conceptualization, Methodology, Formal analysis, Writing—original draft. L.G.: Methodology, Formal analysis, Writing—original draft. N.R.S.: Methodology, Formal analysis, Writing—original draft. N.E.V.: Methodology, Writing—original draft. B.G.N.: Funding acquisition, Writing—review and editing. J.G.P.: Investigation, Writing—review and editing. R.A.: Investigation, Formal analysis. S.S.N.: Conceptualization, Investigation, Supervision, Funding acquisition and Writing—review and editing. All authors have read and agreed to the published version of the manuscript.

Funding: The authors gratefully acknowledge the financial support provided to Sandra San through a fellowship awarded under the Amrita Seed Grant Scheme. Sudarslal Sadasivan Nair acknowledges Amrita Vishwa Vidyapeetham for supporting this research through the Amrita Seed Grant Scheme (Order No. ASG2022068). The authors gratefully acknowledge Sri Mata Amritanandamayi Devi

(Amma), Chancellor, Amrita Vishwa Vidyapeetham, for her inspiration and for providing financial support for the article processing charges (APC) of this publication.

Institutional Review Board Statement: Not applicable.

Informed Consent Statement: Not applicable.

Data Availability Statement: The data supporting the findings of this study are available from the corresponding author upon request.

Acknowledgments: The authors gratefully acknowledge the Amrita Seed Grant Scheme for providing the infrastructure and financial support necessary to conduct this research. The authors also acknowledge the DBT-SAHAJ National Facility for Mass Spectrometry, BRIC-Rajiv Gandhi Centre for Biotechnology (RGCB), Thiruvananthapuram, Kerala, for carrying out proteomic profiling of the purified protein using liquid chromatography-tandem mass spectrometry (LC-MS/MS). The authors acknowledge that a patent application related to the data described in this study has been published by the Indian patent office on 03 July 2026 (Application No. 202541062749). Declaration of generative AI and AI-assisted technologies in the writing process: During the preparation of this work, the authors used ChatGPT (GPT-6, OpenAI) and Google Gemini to assist with rephrasing and improving the quality of sentences. Following the use of these tools, the authors reviewed and edited the content as necessary and take full responsibility for the content of the published article.

Conflicts of Interest: The authors declare there is no conflict of interest.

References

1. Paul, S.; Das, S. Natural insecticidal proteins, the promising bio-control compounds for future crop protection. *Nucleus* **2021**, *64*, 7–20. [CrossRef]
2. Vachon, V.; Laprade, R.; Schwartz, J.-L. Current models of the mode of action of Bacillus thuringiensis insecticidal crystal proteins: A critical review. *J. Invertebr. Pathol.* **2012**, *111*, 1–12. [CrossRef] [PubMed]
3. Carlini, C.R.; Grossi-de-Sá, M.F. Plant toxic proteins with insecticidal properties. A review on their potentialities as bioinsecticides. *Toxicon* **2002**, *40*, 1515–1539. [CrossRef] [PubMed]
4. Rodríguez-Sifuentes, L.; Marszalek, J.E.; Chuck-Hernández, C.; Serna-Saldívar, S.O. Legumes protease inhibitors as biopesticides and their defense mechanisms against biotic factors. *Int. J. Mol. Sci.* **2020**, *21*, 3322. [CrossRef] [PubMed]
5. Richardson, M.J. Seed storage proteins: The enzyme inhibitors. In *Methods in Plant Biochemistry*; Academic Press: New York, NY, USA, 1991; pp. 259–305.
6. Nawaz, A.; Sufyan, M.; Tayyab, M.; Ejaz, A.; Qayyum, M.A.; Waseem, M.; Gogi, M.D.; Arif, M.J.; Munawar, A.; Zhou, W. Role of Protease Inhibitors in Recent Trends of Insect. In *Advances in Integrated Pest Management Technology: Innovative and Applied Aspects*; Springer International Publishing: Berlin/Heidelberg, Germany, 2022; pp. 271–296. [CrossRef]
7. Haq, S.K.; Atif, S.M.; Khan, R.H. Protein proteinase inhibitor genes in combat against insects, pests, and pathogens: Natural and engineered phytoprotection. *Arch. Biochem. Biophys.* **2004**, *431*, 145–159. [CrossRef] [PubMed]
8. Zhu-Salzman, K.; Zeng, R. Insect Response to Plant Defensive Protease Inhibitors. *Annu. Rev. Entomol.* **2015**, *60*, 233–252. [CrossRef] [PubMed]
9. Barros, R.d.A.; Meriño-Cabrera, Y.; Castro, J.S.; Junior, N.R.d.S.; de Oliveira, J.V.A.; Schultz, H.; de Andrade, R.J.; de Oliveira Ramos, H.J.; de Almeida Oliveira, M.G. Bovine pancreatic trypsin inhibitor and soybean Kunitz trypsin inhibitor: Differential effects on proteases and larval development of the soybean pest Anticarsia gemmatalis (Lepidoptera: Noctuidae). *Pestic. Biochem. Physiol.* **2022**, *187*, 105188. [CrossRef] [PubMed]
10. McManus, M.T.; Burgess, E.; Philip, B.; Watson, L.M.; Laing, W.; Voisey, C.R.; White, D.W. Expression of the soybean (Kunitz) trypsin inhibitor in transgenic tobacco: Effects on larval development of Spodoptera litura. *Transgenic Res.* **1999**, *8*, 383–395. [CrossRef]
11. Fonseca, S.S.; Santos, A.L.Z.; Pinto, C.P.G.; Marques, L.; Santos, A.C.; Bing, J.; Nowatzki, T.; Sethi, A.; Rossi, G.D. A soybean trypsin inhibitor reduces the resistance to transgenic maize in a population of *Spodoptera frugiperda* (Lepidoptera: Noctuidae). *J. Econ. Entomol.* **2023**, *116*, 2146–2153. [CrossRef] [PubMed]
12. Shukla, S.; Arora, R.; Sharma, H.C. Biological Activity of Soybean Trypsin Inhibitor and Plant Lectins against Cotton Bollworm/Legume Pod Borer, Helicoverpa armigera. *Plant Biotechnol.* **2005**, *22*, 1–6. [CrossRef]
13. Kanost, M.R.; Jiang, H. Clip-domain serine proteases as immune factors in insect hemolymph. *Curr. Opin. Insect Sci.* **2015**, *11*, 47–55. [CrossRef] [PubMed]
14. Kanost, M.R. Serine proteinase inhibitors in arthropod immunity. *Dev. Comp. Immunol.* **1999**, *23*, 291–301. [CrossRef] [PubMed]

15. Copolovici, D.M.; Langel, K.; Eriste, E.; Langel, Ü. Cell-Penetrating Peptides: Design, Synthesis, and Applications. *ACS Nano* **2014**, *8*, 1972–1994. [CrossRef] [PubMed]
16. Crombez, L.; Aldrian-Herrada, G.; Konate, K.; Nguyen, Q.N.; McMaster, G.K.; Brasseur, R.; Heitz, F.; Divita, G. A new potent secondary amphipathic cell-penetrating peptide for siRNA delivery into mammalian cells. *Mol. Ther.* **2009**, *17*, 95–103. [CrossRef] [PubMed]
17. Joliot, A.; Pernelle, C.; Deagostini-Bazin, H.; Prochiantz, A. Antennapedia homeobox peptide regulates neural morphogenesis. *Proc. Natl. Acad. Sci. USA* **1991**, *88*, 1864–1868. [CrossRef] [PubMed]
18. Derossi, D.; Chassaing, G.; Prochiantz, A. Trojan peptides: The penetratin system for intracellular delivery. *Trends Cell Biol.* **1998**, *8*, 84–87. [CrossRef]
19. Dupont, E.; Prochiantz, A.; Joliot, A. Penetratin Story: An Overview. In *Methods in Molecular Biology*; Humana Press Inc.: Totowa, NJ, USA, 2011; pp. 21–29. [CrossRef] [PubMed]
20. Åmand, H.L.; Fant, K.; Nordén, B.; Esbjörner, E.K. Stimulated endocytosis in penetratin uptake: Effect of arginine and lysine. *Biochem. Biophys. Res. Commun.* **2008**, *371*, 621–625. [CrossRef] [PubMed]
21. Letoha, T.; Gaál, S.; Somlai, C.; Czajlik, A.; Perczel, A.; Penke, B. Membrane translocation of penetratin and its derivatives in different cell lines. *J. Mol. Recognit.* **2003**, *16*, 272–279. [CrossRef] [PubMed]
22. Arai, R.; Ueda, H.; Kitayama, A.; Kamiya, N.; Nagamune, T. Design of the linkers which effectively separate domains of a bifunctional fusion protein. *Protein Eng. Des. Sel.* **2001**, *14*, 529–532. [CrossRef] [PubMed]
23. George, R.A.; Heringa, J. An analysis of protein domain linkers: Their classification and role in protein folding. *Protein Eng. Des. Sel.* **2002**, *15*, 871–879. [CrossRef] [PubMed]
24. Argos, P. An investigation of oligopeptides linking domains in protein tertiary structures and possible candidates for general gene fusion. *J. Mol. Biol.* **1990**, *211*, 943–958. [CrossRef] [PubMed]
25. Gong, Z.; Walls, M.T.; Karley, A.N.; Karlsson, A.J. Effect of a Flexible Linker on Recombinant Expression of Cell-Penetrating Peptide Fusion Proteins and Their Translocation into Fungal Cells. *Mol. Biotechnol.* **2016**, *58*, 838–849. [CrossRef] [PubMed]
26. Hanahan, D. Studies on transformation of Escherichia coli with plasmids. *J. Mol. Biol.* **1983**, *166*, 557–580. [CrossRef] [PubMed]
27. Singh, S.M.; Panda, A.K. Solubilization and refolding of bacterial inclusion body proteins. *J. Biosci. Bioeng.* **2005**, *99*, 303–310. [CrossRef] [PubMed]
28. Mirhosseini, S.A.; Latifi, A.M.; Hosseini, H.M.; Seidmoradi, R.; Aghamollaei, H.; Farnoosh, G. The Efficient Solubilization and Refolding of Recombinant Organophosphorus Hydrolyses Inclusion Bodies Produced in *Escherichia coli*. *J. Appl. Biotechnol. Rep.* **2019**, *6*, 20–25. [CrossRef]
29. Bradford, M.M. A rapid and sensitive method for the quantitation of microgram quantities of protein utilizing the principle of protein-dye binding. *Anal. Biochem.* **1976**, *72*, 248–254. [CrossRef] [PubMed]
30. Herwade, A.P.; Kasar, S.S.; Rane, N.R.; Ahmed, S.; Maras, J.S.; Pawar, P.K. Characterization of a Bowman–Birk type trypsin inhibitor purified from seeds of Solanum surattense. *Sci. Rep.* **2021**, *11*, 8648. [CrossRef] [PubMed]
31. Vanuopadath, M.; Raveendran, D.; Nair, B.G.; Nair, S.S. Venomics and antivenomics of Indian spectacled cobra (Naja naja) from the Western Ghats. *Acta Trop.* **2022**, *228*, 106324. [CrossRef] [PubMed]
32. Nair, D.; Krishna, J.G.; Panikkar, M.V.N.; Nair, B.G.; Pai, J.G.; Nair, S.S. Identification, purification, biochemical and mass spectrometric characterization of novel phycobiliproteins from a marine red alga, Centroceras clavulatum. *Int. J. Biol. Macromol.* **2018**, *114*, 679–691. [CrossRef] [PubMed]
33. Featherstone, D.E.; Chen, K.; Broadie, K. Harvesting and Preparing Drosophila Embryos for Electrophysiological Recording and Other Procedures. *J. Vis. Exp.* **2009**, *27*, 1347. [CrossRef] [PubMed]
34. Rand, M.D.; Montgomery, S.L.; Prince, L.; Vorojeikina, D. Developmental Toxicity Assays Using the *Drosophila* Model. *Curr. Protoc. Toxicol.* **2014**, *59*, 1.12.1–1.12.20. [CrossRef] [PubMed]
35. Rockwell, A.L.; Beaver, I.; Hongay, C.F. A Direct and Simple Method to Assess Drosophila melanogaster's Viability from Embryo to Adult. *J. Vis. Exp.* **2019**. [CrossRef] [PubMed]
36. Nichols, C.D.; Becnel, J.; Pandey, U.B. Methods to Assay Drosophila Behavior. *J. Vis. Exp.* **2012**. [CrossRef] [PubMed]
37. Fellner, A.; Bresgen, N.; Fefer, M.; Liu, J.; Plaetzer, K. Fly into the light: Eliminating Drosophila melanogaster with chlorophyllin-based Photodynamic Inactivation. *Photochem. Photobiol. Sci.* **2024**, *23*, 1155–1166. [CrossRef] [PubMed]
38. Kim, S.-H.; Hara, S.; Hase, S.; Ikenaka, T.; Toda, H.; Kitamura, K.; Kaizuma, N. Comparative Study on Amino Acid Sequences of Kunitz-Type Soybean Trypsin Inhibitors, Tia, Tib, and Tic1. *J. Biochem.* **1985**, *98*, 435–448. [CrossRef] [PubMed]
39. Zhao, A.; Li, Y.; Leng, C.; Wang, P.; Li, Y. Inhibitory effect of protease inhibitors on larval midgut protease activities and the performance of Plutella xylostella (Lepidoptera: Plutellidae). *Front. Physiol.* **2019**, *9*, 1963. [CrossRef] [PubMed]
40. McManus, M.T.; Burgess, E. Effects of the soybean (Kunitz) trypsin inhibitor on growth and digestive proteases of larvae of Spodoptera litura. *J. Insect Physiol.* **1995**, *41*, 731–738. [CrossRef]
41. Johnston, K.; Gatehouse, J.; Anstee, J. Effects of soybean protease inhibitors on the growth and development of larval Helicoverpa armigera. *J. Insect Physiol.* **1993**, *39*, 657–664. [CrossRef]

42. Wu, W.; Ali, A.; Shen, J.; Ren, M.; Cai, Y.; He, L. Cell Penetrating Peptide Enhances the Aphidicidal Activity of Spider Venom-Derived Neurotoxin. *Toxins* **2024**, *16*, 358. [CrossRef] [PubMed]
43. Zhu, Q.; Chen, Z.; Paul, P.K.; Lu, Y.; Wu, W.; Qi, J. Oral delivery of proteins and peptides: Challenges, status quo and future perspectives. *Acta Pharm. Sin. B* **2021**, *11*, 2416–2448. [CrossRef] [PubMed]
44. Gill, R.; Valdes, J.; Bentley, W. A Comparative Study of Global Stress Gene Regulation in Response to Overexpression of Recombinant Proteins in Escherichia coli. *Metab. Eng.* **2000**, *2*, 178–189. [CrossRef] [PubMed]
45. Zeng, H.; Yang, A. Quantification of proteomic and metabolic burdens predicts growth retardation and overflow metabolism in recombinant *Escherichia coli*. *Biotechnol. Bioeng.* **2019**, *116*, 1484–1495. [CrossRef] [PubMed]
46. Hannig, G.; Makrides, S.C. Strategies for Optimizing Heterologous Protein Expression in *Escherichia coli*. *Trends Biotechnol.* **1998**, *16*, 54–60. [CrossRef] [PubMed]
47. Xu, Y.; Zhang, P.; Liu, X.; Wang, Z.; Li, S. Preparation and Irreversible Inhibition Mechanism Insight into a Recombinant Kunitz Trypsin Inhibitor from *Glycine max* L. Seeds. *Appl. Biochem. Biotechnol.* **2020**, *191*, 1207–1222. [CrossRef] [PubMed]
48. Jacob, J.; Meethal, K.V. Gene Cloning, Expression, and Purification of Kunitz Trypsin Inhibitor from Glycine max Using Halo Tag. *Mol. Biotechnol.* **2026**, *68*, 1–12. [CrossRef] [PubMed]
49. Castillo-Corujo, A.; Uchida, Y.; Saaranen, M.J.; Ruddock, L.W. *Escherichia coli* Cytoplasmic Expression of Disulfide-Bonded Proteins: Side-by-Side Comparison between Two Competing Strategies. *J. Microbiol. Biotechnol.* **2024**, *34*, 1126–1134. [CrossRef] [PubMed]
50. Delaunay-Moisan, A.; Ponsero, A.; Toledano, M.B. Reexamining the Function of Glutathione in Oxidative Protein Folding and Secretion. *Antioxid. Redox Signal.* **2017**, *27*, 1178–1199. [CrossRef] [PubMed]
51. Knoke, L.R.; Zimmermann, J.; Lupilov, N.; Schneider, J.F.; Celebi, B.; Morgan, B.; Leichert, L.I. The role of glutathione in periplasmic redox homeostasis and oxidative protein folding in Escherichia coli. *Redox Biol.* **2023**, *64*, 102800. [CrossRef] [PubMed]
52. Wang, S.-S.; Chang, C.-K.; Peng, M.-J.; Liu, H.-S. Effect of glutathione redox system on lysozyme refolding in size exclusion chromatography. *Food Bioprod. Process.* **2006**, *84*, 18–27. [CrossRef]
53. Oyeleye, A.O.; Yusoff, S.F.M.; Rahim, I.N.A.; Leow, A.T.C.; Saidi, N.B.; Normi, Y.M. Effective refolding of a cysteine rich glycoside hydrolase family 19 recombinant chitinase from Streptomyces griseus by reverse dilution and affinity chromatography. *PLoS ONE* **2020**, *15*, e0241074. [CrossRef] [PubMed]
54. Vlaskina, A.; Petrenko, D.; Agapova, Y.; Kuzminkova, A.; Evteeva, M.; Patrushev, M. On-Column Dual-Gradient Refolding for Efficient Recovery of Insoluble Affinity-Tagged Recombinant Proteins. *Bio-Protocol* **2026**, *16*, e5598. [CrossRef] [PubMed]
55. Dong, X.-Y.; Chen, L.-J.; Sun, Y. Effect of operating conditions on the refolding of his-tagged enhanced green fluorescent protein by artificial chaperone-assisted metal affinity chromatography. *Biochem. Eng. J.* **2009**, *48*, 65–70. [CrossRef]
56. Carson, M.; Johnson, D.H.; McDonald, H.; Brouillette, C.; DeLucas, L.J. His-tag impact on structure. *Acta Crystallogr. Sect. D Struct. Biol.* **2007**, *63*, 295–301. [CrossRef] [PubMed]
57. Booth, W.T.; Schlachter, C.R.; Pote, S.; Ussin, N.; Mank, N.J.; Klapper, V.; Offermann, L.R.; Tang, C.; Hurlburt, B.K.; Chruszcz, M. Impact of an N-terminal Polyhistidine Tag on Protein Thermal Stability. *ACS Omega* **2018**, *3*, 760–768. [CrossRef] [PubMed]
58. Majorek, K.A.; Kuhn, M.L.; Chruszcz, M.; Anderson, W.F.; Minor, W. Double trouble—Buffer selection and His-tag presence may be responsible for nonreproducibility of biomedical experiments. *Protein Sci.* **2014**, *23*, 1359–1368. [CrossRef] [PubMed]
59. Dau, T.; Bartolomucci, G.; Rappsilber, J. Proteomics Using Protease Alternatives to Trypsin Benefits from Sequential Digestion with Trypsin. *Anal. Chem.* **2020**, *92*, 9523–9527. [CrossRef] [PubMed]
60. Jamal, F.; Pandey, P.K.; Singh, D.; Ahmed, W. A Kunitz-type serine protease inhibitor from Butea monosperma seed and its influence on developmental physiology of Helicoverpa armigera. *Process Biochem.* **2015**, *50*, 311–316. [CrossRef]
61. Cermenati, G.; Terracciano, I.; Castelli, I.; Giordana, B.; Rao, R.; Pennacchio, F.; Casartelli, M. The CPP Tat enhances eGFP cell internalization and transepithelial transport by the larval midgut of Bombyx mori (Lepidoptera, Bombycidae). *J. Insect Physiol.* **2011**, *57*, 1689–1697. [CrossRef] [PubMed]
62. Sukiran, N.A.; Pyati, P.; E Willis, C.; Brown, A.P.; Readshaw, J.J.; Fitches, E.C. Enhancing the oral and topical insecticidal efficacy of a commercialized spider venom peptide biopesticide via fusion to the carrier snowdrop lectin (*Galanthus nivalis* agglutinin). *Pest Manag. Sci.* **2023**, *79*, 284–294. [CrossRef] [PubMed]
63. Hughes, S.R.; Dowd, P.F.; Johnson, E.T. Cell-penetrating recombinant peptides for potential use in agricultural pest control applications. *Pharmaceuticals* **2012**, *5*, 1054–1063. [CrossRef] [PubMed]
64. Takenaka, A.; Konno, H.; Kikuta, S. In vivo direct cell-penetrating peptide mediated protein transduction system in Acyrthosiphon pisum. *BMC Res. Notes* **2023**, *16*, 231. [CrossRef] [PubMed]

Disclaimer/Publisher's Note: The statements, opinions and data contained in all publications are solely those of the individual author(s) and contributor(s) and not of MDPI and/or the editor(s). MDPI and/or the editor(s) disclaim responsibility for any injury to people or property resulting from any ideas, methods, instructions or products referred to in the content.